# A review: Photonics devices, architectures, and algorithms for optical neural computing

**Shuiying Xiang[1, 2, †], Yanan Han[1], Ziwei Song[1], Xingxing Guo[1], Yahui Zhang[1], Zhenxing Ren[1], Suhong Wang[1], Yuanting Ma[1], Weiwen Zou[3], Bowen Ma[3], Shaofu Xu[3], Jianji Dong[4], Hailong Zhou[4], Quansheng Ren[5], Tao Deng[6], Yan Liu[2], Genquan Han[2], and Yue Hao[2]**

[1]State Key Laboratory of Integrated Service Networks, Xidian University, Xi'an 710071, China

[2]State Key Discipline Laboratory of Wide Bandgap Semiconductor Technology, School of Microelectronics, Xidian University, Xi'an 710071, China

[3]State Key Laboratory of Advanced Optical Communication Systems and Networks, Intelligent Microwave Lightwave Integration Innovation Center (iMLic), Department of Electronic Engineering, Shanghai Jiao Tong University, Shanghai 200240, China

[4]Wuhan National Laboratory for Optoelectronics, School of Optical and Electronic Information, Huazhong University of Science and Technology, Wuhan 430074, China

[5]School of Electronics Engineering and Computer Science, Peking University, Beijing 100871, China

[6]School of Physical Science and Technology, Southwest University, Chongqing 400715, China

**Abstract:** The explosive growth of data and information has motivated various emerging non-von Neumann computational approaches in the More-than-Moore era. Photonics neuromorphic computing has attracted lots of attention due to the fascinating advantages such as high speed, wide bandwidth, and massive parallelism. Here, we offer a review on the optical neural computing in our research groups at the device and system levels. The photonics neuron and photonics synapse plasticity are presented. In addition, we introduce several optical neural computing architectures and algorithms including photonic spiking neural network, photonic convolutional neural network, photonic matrix computation, photonic reservoir computing, and photonic reinforcement learning. Finally, we summarize the major challenges faced by photonic neuromorphic computing, and propose promising solutions and perspectives.

**Key words:** photonics neuron; photonic STDP; photonic spiking neural network; optical reservoir computing; optical convolutional neural network; neuromorphic photonics

## 1. Introduction

In the past few decades, the computing capability of conventional digital computers based on complementary metal oxide semiconductor (CMOS) transistors has been increased greatly as predicted by Gordon Moore[1]. With the rapid development of artificial intelligence (AI) and internet of things, an exponential growth in the amount of data has led to urgent requirements for high efficiency and ultralow power consumption for the data-centric applications. In a standard digital computer based on the von Neumann architecture, the memory and processor are physically separated. Significant data movement between memory and processor is costly in terms of time and energy in today's von Neumann systems. Meanwhile, Moore's law has been slowing down significantly in recent years[2]. Thus, innovative non-von Neumann computational approaches are highly desired in the More-than-Moore era.

The human brain, which is believed to be the most complex intelligent system in the universe, exhibits ultralow power consumption, massive parallelism, robust fault tolerance, self-adaptation, and self-learning ability. The architecture of the human brain differs from that of a digital computer. Generally, a biological neural network is composed of roughly $10^{11}$ neurons and $10^{15}$ synapses, and is normally represented by spiking neural network (SNN)[3]. In the brain, the information is represented and transmitted by action potential, i.e., spike[4, 5]. The spike signals transmitted between the neurons connected through synapses with synaptic plasticity. Spike timing-dependent plasticity (STDP) is one of the most widely studied synaptic plasticity mechanism[6–8].

Inspired by the network architecture and principles of the human brain, the neuromorphic computing system has drawn tremendous attention in the next generation of computing technology. Nowadays, both the digital and analog hardware paradigms based on the CMOS technologies have been fully developed[9, 10]. In addition, extensive efforts have also been made to mimic the functions of biological neurons and synapses by various electronic neuromorphic devices. In recent years, remarkable progress has been made from materials to devices, circuits, and architectures in the field of electronic neuromorphic computing[9–12]. However, the operation speed of the electronic neuromorphic computing system is
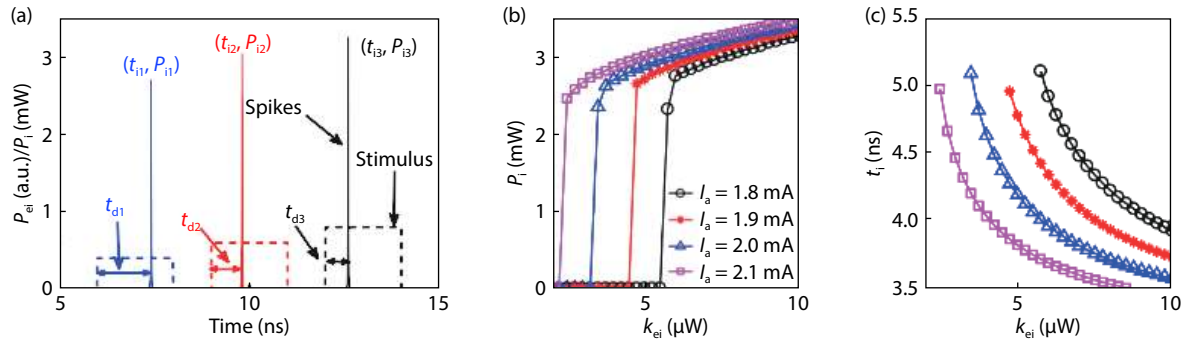
Fig. 1. (Color online) (a) Temporal output of the spike encoding based on the modeling-based photonic neuron. (b) Threshold-like response and (c) spike latency property of the modeling-based photonic neuron. © [2020] IEEE. Reprinted with permission from Ref. [39].

restricted due to the bandwidth–connection density trade-off[13].

As a complementary approach, the photonics platform has gained increasing attention for hardware neuromorphic computing, due to the fascinating advantages such as high speed, wide bandwidth, and massive parallelism. The photonics neuromorphic computing shows great promise in the applications which require low latency, low power consumption, and high bandwidth. Nevertheless, the photonics neuromorphic computing is still in its infancy compared to the electronics counterpart. Nahmias et al. proposed a photonic leaky integrate-and-fire (LIF) neuron based on vertical-cavity surface-emitting lasers with saturable absorber (VCSELs-SA)[14]. With the help of Yamada model, the neuron-like spiking dynamics was reproduced in the VCSEL-SA model. On the other hand, there are also some proposed photonics synapses. For instance, Gholipour et al. developed photonic synapses based on amorphous gallium lanthanum oxysulphide microfibers[15]. Cheng et al. fabricated and demonstrated an on-chip photonic synapse via phase-change materials combined with integrated silicon nitride waveguide[16]. Specifically, Feldmann et al. implemented an all-optical SNN with self-learning capacity based on a nanophotonic chip, and successfully demonstrated supervised and unsupervised learning in the optical domain[17]. For more detail on the spiking neurons and synapses based on photonic devices, please refer to Refs. [13, 18–21].

Generally, the photonics neurons and synapses are studied separately with different devices, therefore leading to the need for further developing high-performance photonics neuron and synaptic devices. In addition, algorithm is another key issue that limits the progress of photonic SNN development.

Herein, we review some recent progress on the devices, architecture, and algorithm of photonic neural computing in our research groups. First, we introduce the photonic neuron at the device level. Then, we review the progress on the photonic STDP. Subsequently, we focus on several photonic neural networks at the system level. Finally, we summarize the challenges and opportunities faced by photonic neural computing, and propose promising solutions and perspectives.

## 2. Photonic neuron

Photonic devices operating in the excitable regime are dynamically analogous to the biological neurons exhibit spiking dynamics. While the operating speed of photonic devices are many orders of magnitude faster than their biological counterparts. There are various optical neurons reported experimentally and numerically in recent years[14, 22–39]. Here, we focus on the lasers-based optical neuron. Some recent progress on the optical neurons based on conventional VCSEL, VCSEL-SA, as well as distributed feedback laser (DFB) are reviewed.

### 2.1. Optical neuron based on VCSEL-SA

A VCSEL-SA can be employed as a photonics neuron because it possesses the excitability property behaves analogously to the LIF neuron model. The excitability properties and the spike latency of the VCSELs-SA are shown in Fig. 1[39]. Fig. 1(a) shows that the VCSEL-SA could generate excitatory neuron-like spike and realize the temporal encoding. The spike latency, defined as the interval between the start time of stimulus pulse and the timing corresponding to the maximum value of spikes generated by VCSEL-SA, varied with different stimuli strengths and central timings. As presented in Fig. 1(b), when the stimuli pulse power exceeds a threshold value, the VCSEL-SA can emit a spike. In addition, such threshold behavior can be tuned by different bias current. Fig. 1(c) indicated that the spiking timing can be continuously adjusted by different stimulus strength.

Note, the inhibitory dynamics is also important for the neural information processing. We further revealed the inhibitory dynamics based on the polarization mode competition effect in a VCSEL-SA with two coexisting polarization-resolved modes[33]. The schematic diagram of inhibitory photonic neuron based on VCSEL-SA is presented in Fig. 2(a). The inhibition behavior was characterized by the spike amplitude and first spike latency. As presented in Fig. 2(b), the neuron-like inhibition behavior could be achieved thanks to the polarization mode competition. Furthermore, as presented in Fig. 3, such inhibition dynamics could also be used to realize the spike-based XOR in a single step with a single VCSEL-SA[34]. Additionally, the XOR operation was also achieved successfully with two pseudo-random return-to-zero sequences.

### 2.2. Optical neuron based on VCSEL

The VCSELs have become promising candidates for artificial neuronal models due to the polarization switching or optical injection induced nonlinear dynamics. Recently, the controllable and reproducible excitation and inhibition behaviors at sub-nanosecond speeds for a commercially available VCSEL subject to the successive external stimulus have been experimentally and theoretically demonstrated[22, 24–30, 36]. Under an external injection characterized by a constant optical power
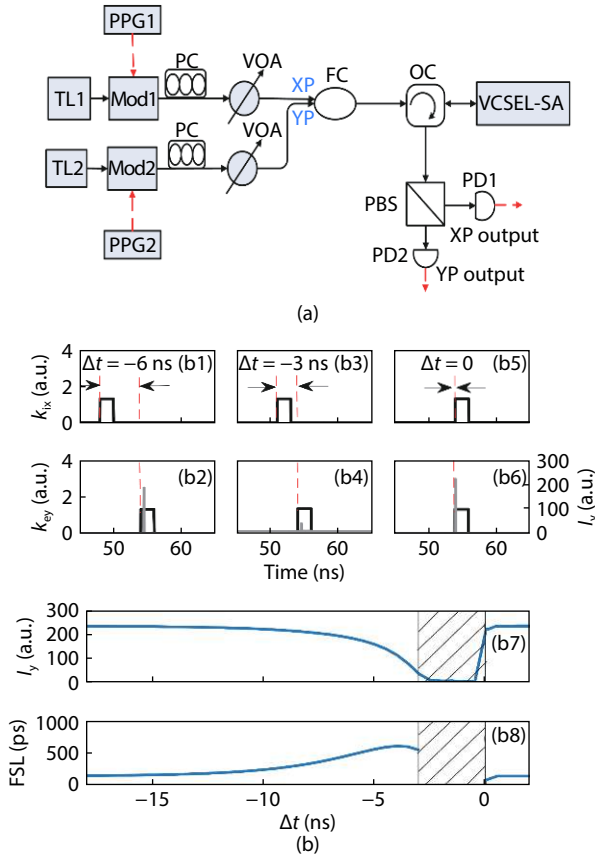
Fig. 2. (a) Schematic diagram of inhibitory neuron based on VSCEL-SA. Reprinted from Ref. [31]. (b) The results of inhibition in a photonic neuron. Reprinted with permission from Ref. [33]. © The Optical Society.

level with sudden perturbation in the form of short power drops, the VCSEL-neuron can transmit from the injection-locking state into the unlocking state after the arrival of the perturbation due to the broken equilibrium and a spiking event is triggered. Moreover, the number of fired spikes can be controlled through adjusting the temporal duration of incoming perturbations, as shown in Figs. 4(b1)–4(b5)[26, 28]. Also, under the external injection in the form of a constant level with sudden power raises for increasing perturbation duration, the spiking regime could be entirely suppressed during the perturbation period, as shown in Figs. 4(c1)–4(c5)[30]. Moreover, the communication of excitatory and inhibitory spiking signals at sub-nanosecond speeds between two coupled VCSEL-neurons have also been demonstrated experimentally and numerically[26–28, 30].

### 2.3. Optical neuron based on DFB

The DFB exhibits similar processing characteristics with the graded-potential-signaling-based neuron observed in the nervous system, such as temporal integration and pulse facilitation. A commercially available DFB was demonstrated to play a role in three applications of neuromorphic information processing for pattern recognition, single-wavelength STDP implementation, and sound azimuth measurement, as shown in Fig. 5[37]. To further investigate the spatiotemporal processing potential of DFB neurons, a network architecture was proposed to be equipped with $N$ tunable weights on each input branch for complex pattern recognition[38]. The schematic of the network is illustrated by Fig. 6(a). Successful pattern recognition was demonstrated among the input sets when

$N$ = 3 and 4, as given in Figs. 6(b) and 6(c), respectively. Additionally, the network can learn a target pattern by the assistance of the STDP learning module also realized by a DFB, which is convenient for the potential integration.

## 3. Photonic synaptic plasticity

In brains, synaptic plasticity is believed to be closely related to the learning and memory. In this section, we review the emulation of the synaptic function based on the semiconductor optical amplifier (SOA) and vertical-cavity semiconductor optical amplifier (VCSOA). The photonic STDP is focused on.

### 3.1. Photonic STDP based on SOA

STDP is a long-term synaptic plasticity observed experimentally in biological synapses by Bi and Poo[6]. Thanks to the cross-gain modulation in SOA, the implementation of optical STDP scheme based on SOA was demonstrated[40–43]. The result in Fig. 7 shows that the STDP curve is similar to that measured in biological experiments, but at a much faster time scale[41]. Moreover, the height and width of the measured STDP learning window decrease as the SOA current increases.

### 3.2. Photonic STDP based on VCSOA

Note that, for the photonic STDP based on SOA, the operation current of SOA is relatively high, i.e., several tens of or hundreds of mA. When operating below threshold, the VCSEL can also be regarded as VCSOA. The photonic STDP based on the VCSOA was proposed and demonstrated experimentally and numerically[44]. The schematic diagram is illustrated in Fig. 8(a). In our experiment, the VCSOA was biased at 1.42 mA, the optical pulse power (width) was 70 $\mu$W (100 ps). The energy consumption for biasing the VCSOA and triggering the STDP function could be estimated as several femtojoules per spike, which is much lower than the microelectronic counterparts[45, 46]. The experimental measurements are shown in Fig. 8(b). When two optical pulses with different time interval were injected into the VCSOA, the lagged pulse experienced different gain due to the carrier depletion caused by the leading pulses. With the increase of time interval, the output power of the lagged pulse increased gradually. The numerical results are presented in Figs. 8(c) and 8(d), which agree well with the experimental measurements. Fig. 8(e) shows that the STDP curve can be achieved in VCSOA with low bias current. The calculated STDP window was about 1 ns, indicating that the STDP operation rate was nearly 1 GHz, which is higher than the conventional electronics[45, 46]. Furthermore, such photonic STDP curve can also be achieved in real-time with a single VCSEL with dual-polarized pulsed optical injection[47].

## 4. Photonic neural computing

In this section, we review the progress on the optical neural computing at the system level. We consider several network architectures and algorithms including photonic SNN, photonic convolutional neural network (CNN), photonic matrix computation, photonic reservoir computing (RC), and photonic reinforcement learning.

### 4.1. Photonic SNN

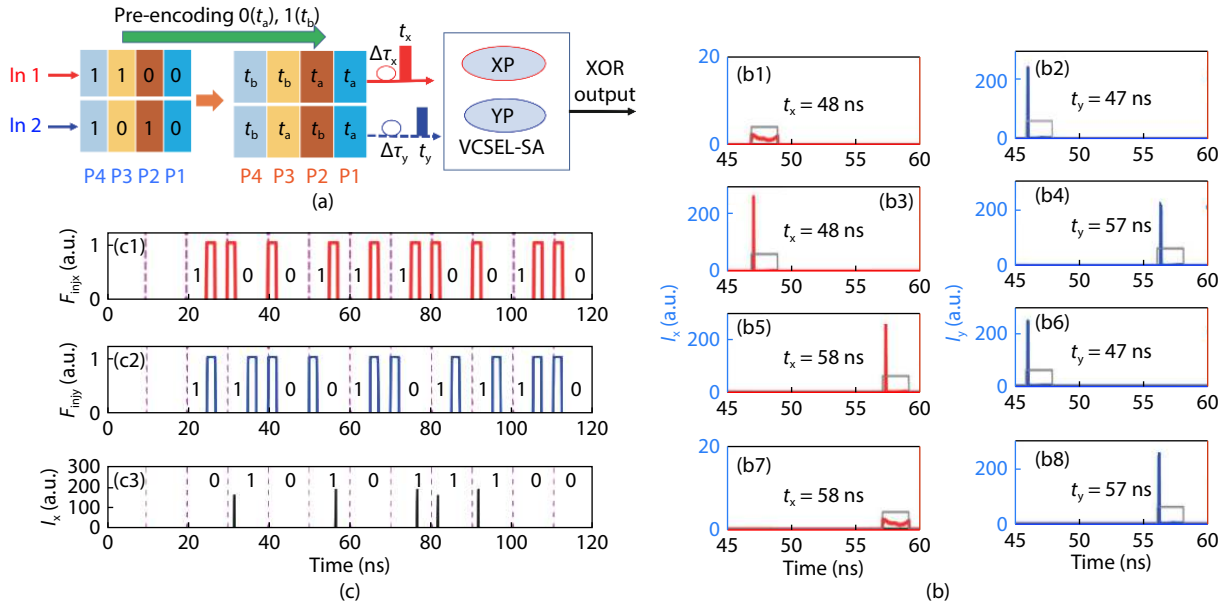To design the algorithm for a photonic SNN, we pro-

Fig. 3. (Color online) (a) Schematic diagram of all-optical exclusive OR (XOR) operator based on a single VCSEL-SA. (b) XOR output for different sets of inputs. (c) The inputs and outputs of XOR for two RZ sequences. Reprinted with permission from Ref. [34]. © The Optical Society.
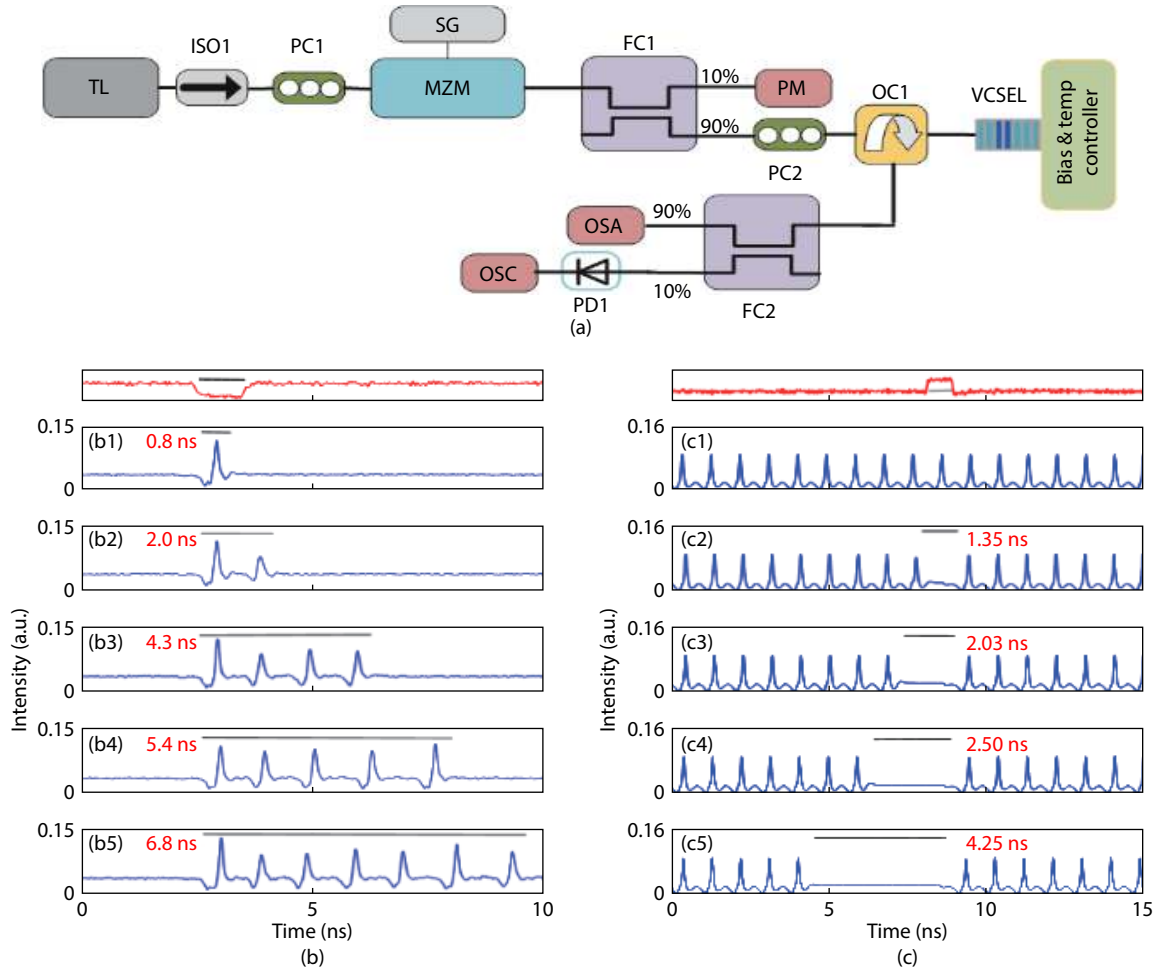


Fig. 4. (Color online) (a) The experimental setup for spiking firing and inhibition of VCSEL-based neuron. © [2018] IEEE. Reprinted with permission from Ref. [30]. (b) Time series of fired spiking responses. Reprinted with permission from Ref. [26]. © The Optical Society. © [2017] IEEE. Reprinted with permission from Ref. [28]. (c) Time series of suppressed spiking response. © [2018] IEEE. Reprinted with permission from Ref. [30].

posed a novel framework of a fully VCSEL-based all-optical SNN and developed a self-consistent unified neuron-synapse-learning model that allows a complete learning-to-inference workflow[35, 39]. The unsupervised learning was implemented in a photonic SNN consisting of VCSELs-SA[35]. The input pattern is encoded into spikes at different timings by different VC-
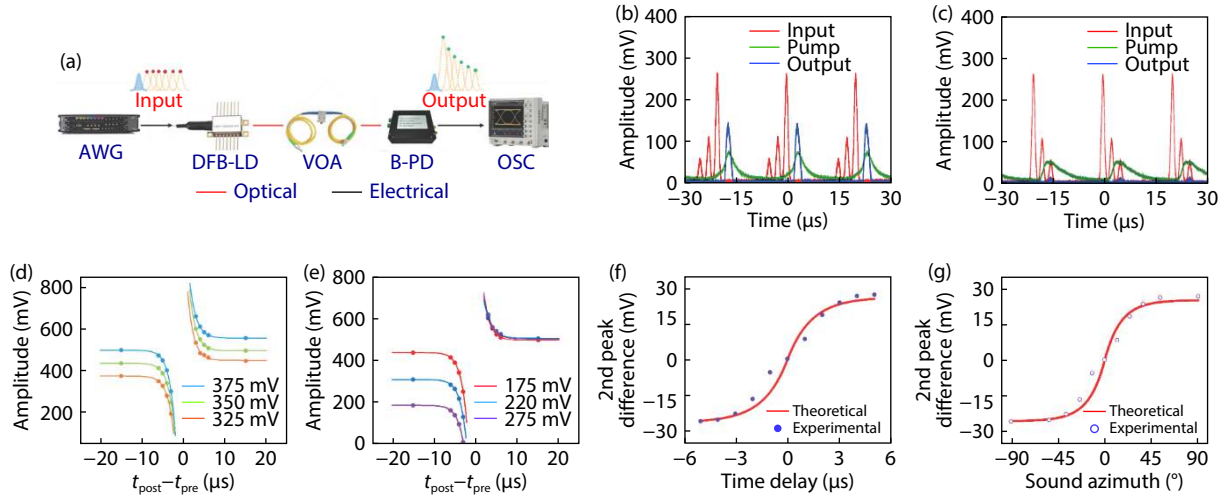
Fig. 5. (Color online) (a) The experimental setup for graded-potential-signaling-based neuromorphic processing applications with the optical neuron based on DFB, including (b, c) pattern recognition, (d, e) single-wavelength implementation of STDP, and (f, g) sound azimuth measurement[37]. Reproduced with permission. © 2020 Springer Nature.
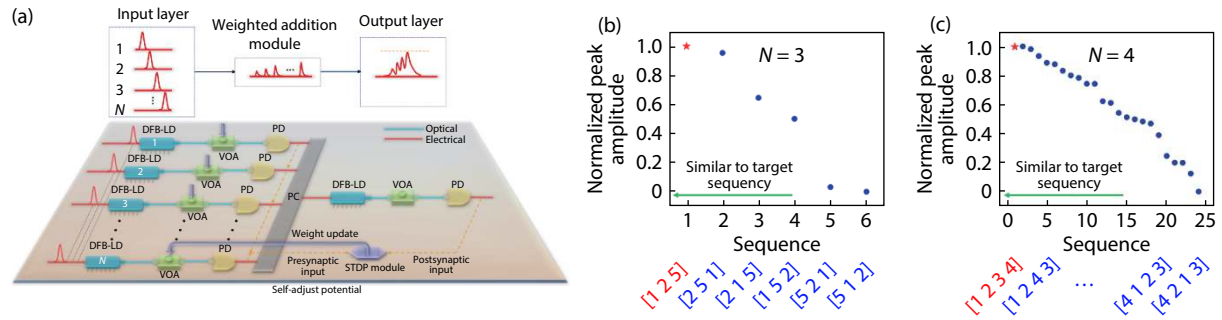


Fig. 6. (Color online) (a) The DFB-based spatiotemporal pattern recognition network with STDP learning module. The network output for patterns with (b) 3 and (c) 4 input branches, respectively. Reprinted with permission from Ref. [38]. © The Optical Society.
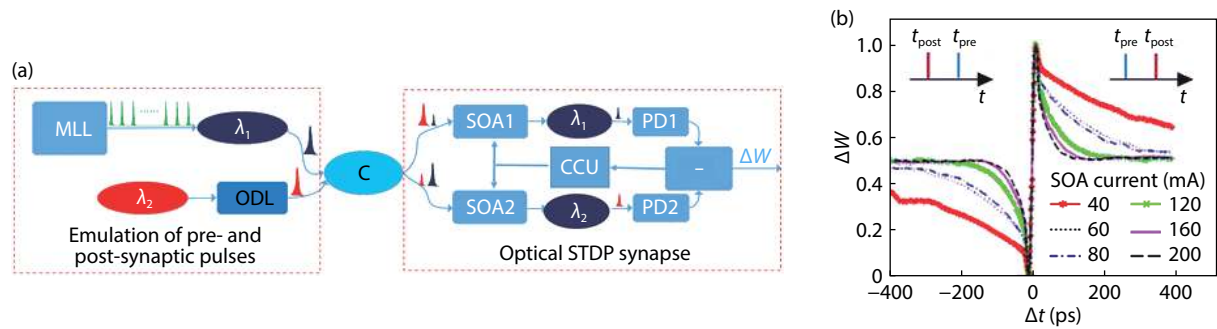


Fig. 7. (Color online) (a) Optical implementation of STDP. (b) The measured learning window of Optical STDP with different SOA driving current. Reprinted with permission from Ref. [41]. © The Optical Society.

SELs-SA. As shown in Fig. 9, the photonic SNN with photonic STDP enables the POST neuron to spike at the first spike timing of the input pattern in an unsupervised manner. In addition, supervised learning was also realized in a photonic SNN[39, 48]. As illustrated in Fig. 10, a supervised spike sequence learning task was implemented in a two-layer fully-connected photonic SNN consisting of excitable VCSELs-SA[48]. In this photonic SNN, the classical remote supervised method (ReSuMe) learning algorithm based on the photonic STDP is adopted to train the POST to fire the desired spike sequence. Fig. 10(c) illustrates the learning process in a typical run. The corresponding spike sequence distance (SSD) as a function of the learning epoch shown in Fig. 10(e) indicates that the learning process was convergent. Therefore, the photonic SNN successfully reproduced a desirable output spike sequence in response to a spatiotemporal input spike pattern by means of the iteration algorithm to update synaptic weights continuously.

The spatiotemporal pattern classification based on supervised learning was further demonstrated based on the spatiotemporal design of the photonic SNN shown in Fig. 11(a)[39]. Optical character numbers were trained and tested by the proposed SNN. As shown in Fig. 11(b), the network was trained with a clean character image, and then, the inference was

**S Y Xiang et al.: A review: Photonics devices, architectures, and algorithms for optical neural computing**
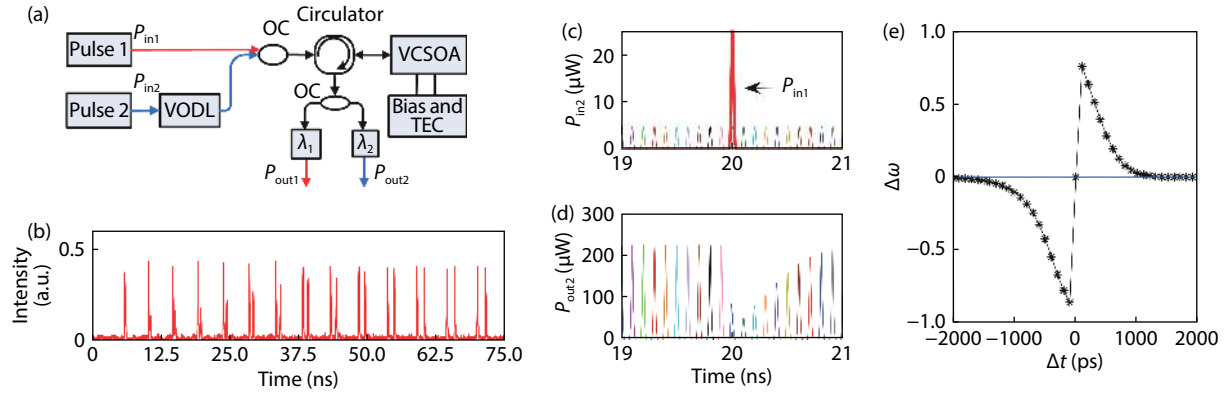
Fig. 8. (Color online) (a) Schematic diagram of photonic STDP based on VCSOA. (b) The experimental measured output pulse train corresponding to the input pulse pairs with different time interval. (c) Simulated input pulse. (d) Simulated output pulse. (e) The calculated STDP curve. Pulse 1 (Pulse 2): the optical pulse injection beam; VODL: variable optical delay line, OC: optical coupler; Circulator: optical circulator; VCSOA: vertical-cavity semiconductor optical amplifier. Bias and TEC: The bias current and temperature controller for VCSOA; $\lambda_{1,2}$ in the box means a band-pass filter. © [2018] IEEE. Reprinted with permission from Ref. [44].
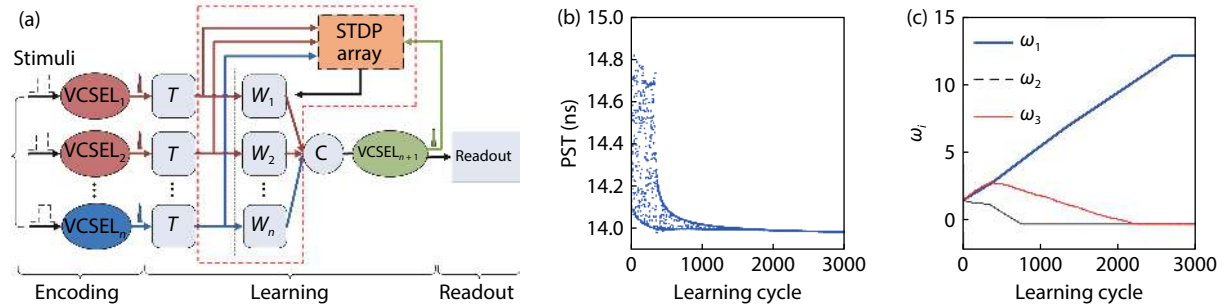


Fig. 9. (Color online) (a) Schematic diagram of photonic SNN based on VCSELs and VCSOAs. (b) PST as a function of the learning cycle. (c) Synaptic weights evolution during the learing process. $n$ photonic presynaptic neurons and one postsynaptic neuron are conneted with optical STDP synapses. VCSEL$_1$–VCSEL$_n$: photonic presynaptic neurons; VCSEL$_{n+1}$: photonic postsynaptic neuron; $T$: variable delay line; $W_i$ ($i = 1, 2, …, n$): variable synaptic weight device connecting VCSEL$_i$ and VCSEL$_{n+1}$; STDP array: optical STDP synapses realized by VCSOAs; C: optical coupler. The red dashed box represents the ex-situ approach for updating the synaptic weight. © [2019] IEEE. Reprinted with permission from Ref. [35].
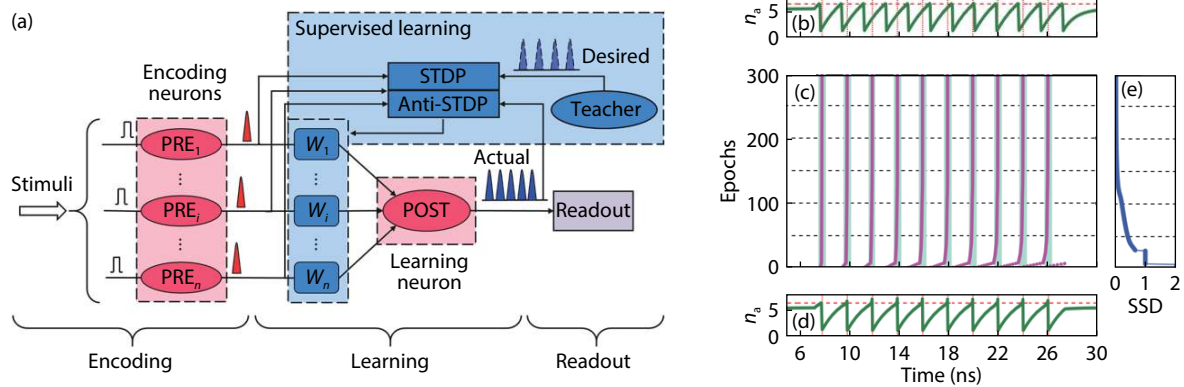


Fig. 10. (Color online) (a) Schematic diagram of a photonic SNN based on VCSEL-SAs for the supervised spike sequence learning. (b-e) Illustration of the spike sequence learning of a typical run. © [2020] IEEE. Reprinted with permission from Ref. [48].

tested with a set of noisy patterns. The results show that this all-optical SNN can recognize ten numbers by a supervised learning algorithm. Besides, the training convergence can be optimized by using different bias current of VCSOA as presented in Fig. 11(c). As illustrated in Fig. 11(d), the accuracy rate of the trained network was robust to small noise strength of the optical digital character.

In addition, sound azimuth detection was emulated in a fully connected photonic SNN consisting of VCSELs-SA[49]. Fig. 12(a) shows the schematic diagram of the proposed photonic SNN which composed of two presynaptic neurons (PREs) considered as the ear sensors, and two postsynaptic neurons (POSTs). The difference between the precise spike timing of two POSTs ($\Delta t_o$) was used as an indication of the
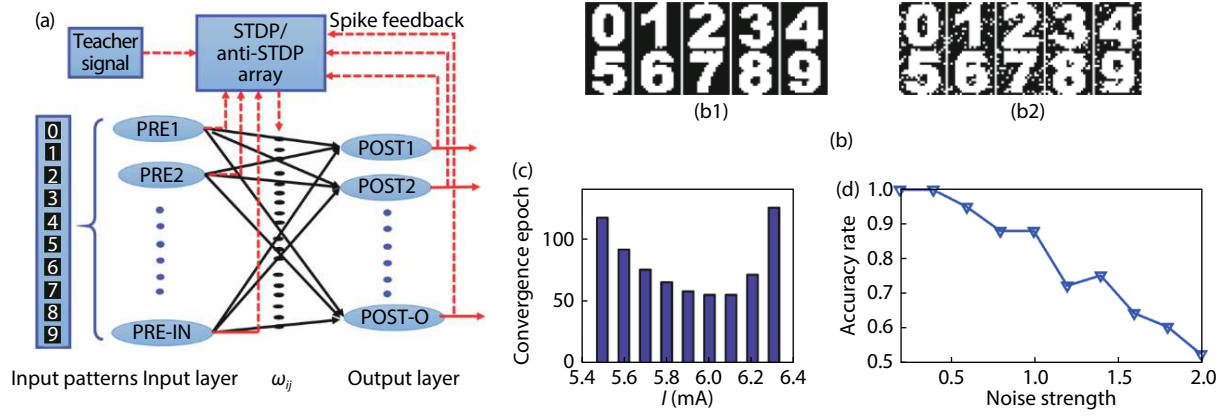
Fig. 11. (Color online) (a) Architecture of the proposed all-optical SNN. (b) An example of a pattern classification task. The network is trained with (b1) a clean character image, and then, the inference was tested with a set of (b2) noisy patterns. (c) Comparison of convergence performance for supervised learning with different I of VCSOA. (d) Accuracy rate of the trained network as a function of the noise strength of the optical digital character. © [2020] IEEE. Reprinted with permission from Ref. [39].
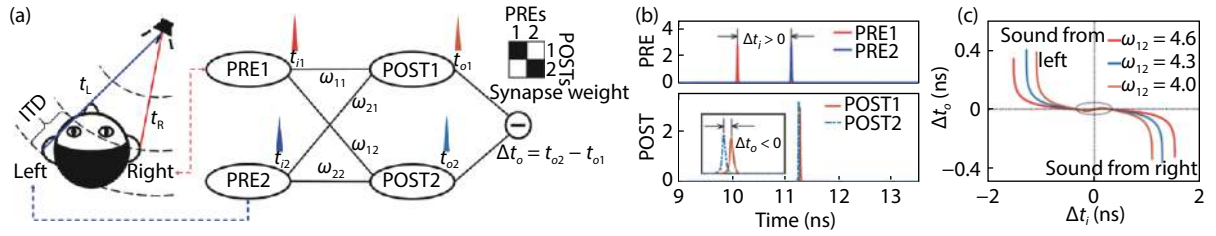


Fig. 12. (a) Schematic structure of a 2 × 2 photonic SNN architecture to detect the sound azimuth, and two PREs correspond to the right ear and left ear, respectively. (b) Responses of POST1 and POST2 when $\Delta t_i < 0$. (c) The calculated $\Delta t_o$ as a function of the $\Delta t_i$ for different weights ($\omega_{12}$). Reprinted with permission from Ref. [49]. © The Optical Society.
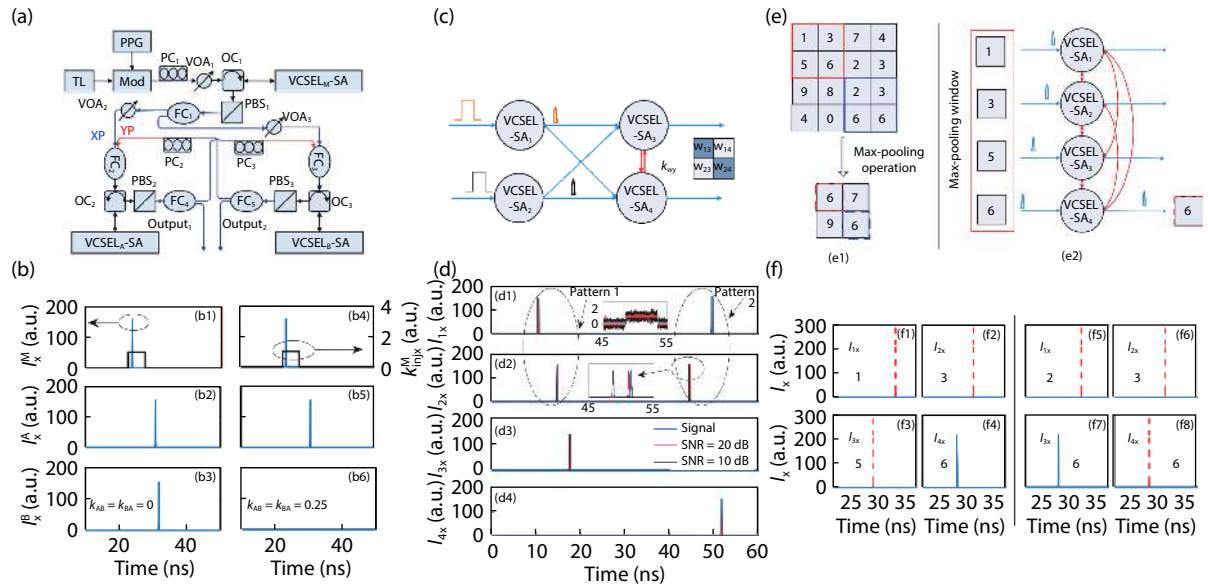


Fig. 13. (Color online) (a) Schematic diagram of WTA based on VCSELs-SA. (b) The output of VCSEL$_{M,A,B}$-SA for WTA mechanism. (c) Schematic diagram of pattern recognition based on the WTA machine. (d) The inputs and results of pattern recognition. (e) Schematic diagram of max-pooling operation. (f) The results of max-pooling operation. © [2020] IEEE. Reprinted with permission from Ref. [50].

sound azimuth. The dependence of $\Delta t_o$ on the relative timing of the spikes of two PREs ($\Delta t_i$) was revealed as illustrated in Fig. 12(b). Furthermore, the effective detection range were identified for different weights as shown in Fig. 12(c). The results demonstrated that the proposed photonic SNN used for

sound azimuth detection was biologically plausible, and has higher resolution compared with the biological system.

Besides, the winner-take-all mechanism was also achieved successfully in the photonic SNN consisting of VCSELs-SA as shown in Figs. 13(a) and 13(b)[50]. Two information pro-
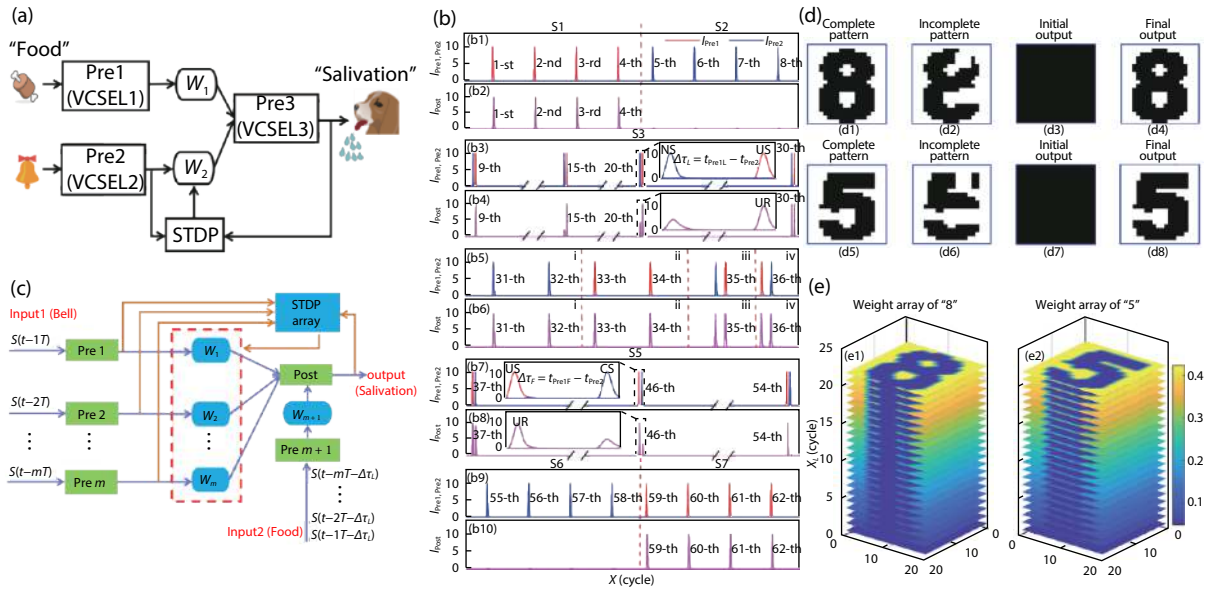
Fig. 14. (Color online) (a) Schematic diagram of associative learning and forgetting processes based on VCSELs and STDP. (b) The emulation of associative learning and forgetting processes. (c) Schematic diagram of pattern recall. (d) Complete and incomplete patterns of number 8 and 5 respectively, visualization initial and final outputs of number 8 and 5 respectively. (e) The change processes of synaptic weight for number 8 and number 5. © [2020] IEEE. Reprinted with permission from Ref. [51].
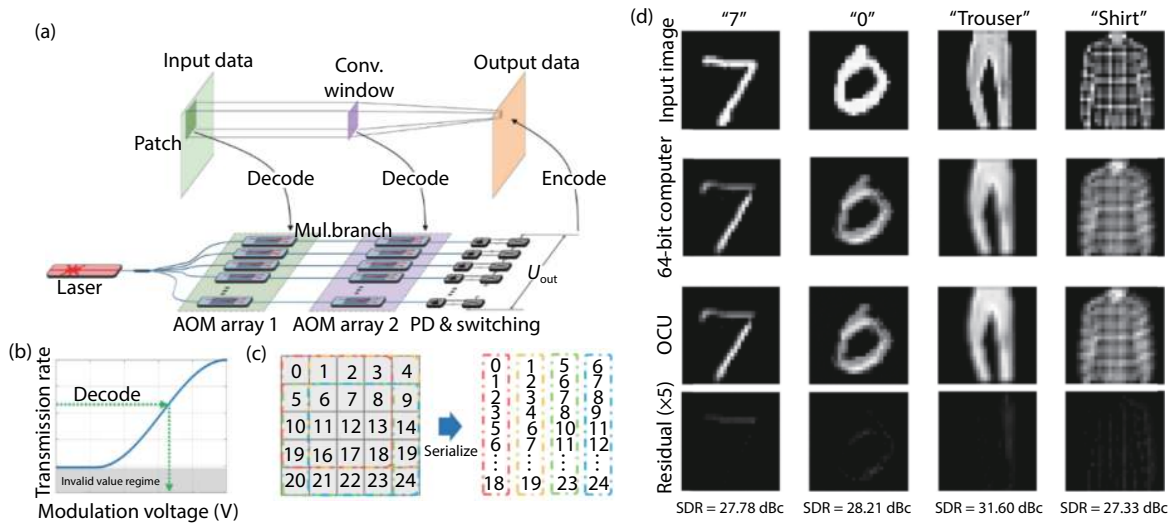


Fig. 15. (Color online) (a) The architecture of the optical convolution unit (OCU) by modulator arrays. (b) The transmission rate versus the modulation voltage of the single modulator. (c) An illustration of the serialization method. (d) The convolution results of MNIST-handwritten numbers and Fashion-MNIST data sets. Reprinted with permission from Ref. [52]. © The Optical Society.

cessing tasks including pattern recognition and max-pooling operation were performed as shown in Figs. 13(c)–13(f). The results hold great promise for the development of energy-efficient and high-speed photonic SNN.

Furthermore, associative learning and forgetting processes were emulated in a photonic SNN[51]. The schematic diagram of the photonic associative learning network is shown in Fig. 14(a). Fig. 14(b) shows that both the associative learning and forgetting processes could be achieved thanks to the photonic STDP rule. The pattern recall based on the associative learning was further demonstrated in the photonic SNN presented in Fig. 14(c). Complete pattern and incomplete pattern of number 8 are shown in Figs. 14(d1) and 14(d2), respectively. Fig. 14(d3) [Fig. 14(d4)] shows the initial output (final out-

put) of number 8 before [after] associative learning process. The evolution of synapse weight corresponding to the pattern recall of number 8 is presented in Fig. 14(e1). Without loss of generality, Figs. 14(d5, d6, d7, d8) and 14(e2) show the pattern recall process of number 5 and the corresponding weight evolution. Obviously, the incomplete pattern can be recovered and pattern recall was realized based on the photonic associative learning network.

### 4.2.  Optical convolutional neural network

The optical implementation of CNN with fast operation speed and high energy efficiency is appealing due to its outstanding feature extraction ability[52–54]. The high-accuracy optical convolution unit (OCU) with cascaded acousto-optical
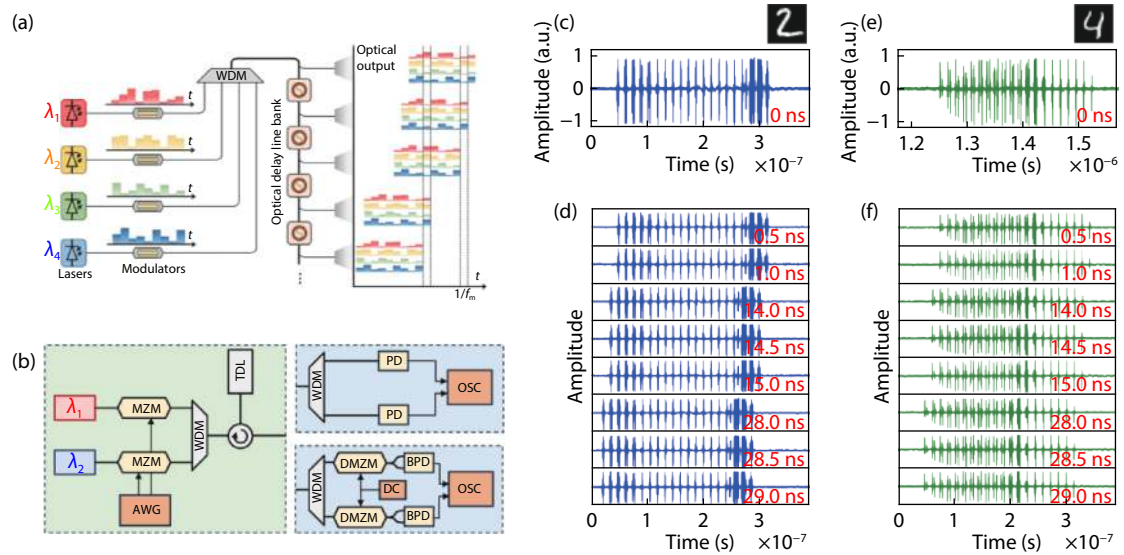
Fig. 16. (Color online) (a) The conceptual layout of the optical patching scheme with optical delay lines and wavelength-division-demultiplexing (WDM). (b) The experimental setup of the proposed scheme. Delayed copies of the input waveforms corresponding to (c, d) digit 2 and (e, f) 4, respectively. Reprinted with permission from Ref. [53]. © The Optical Society.
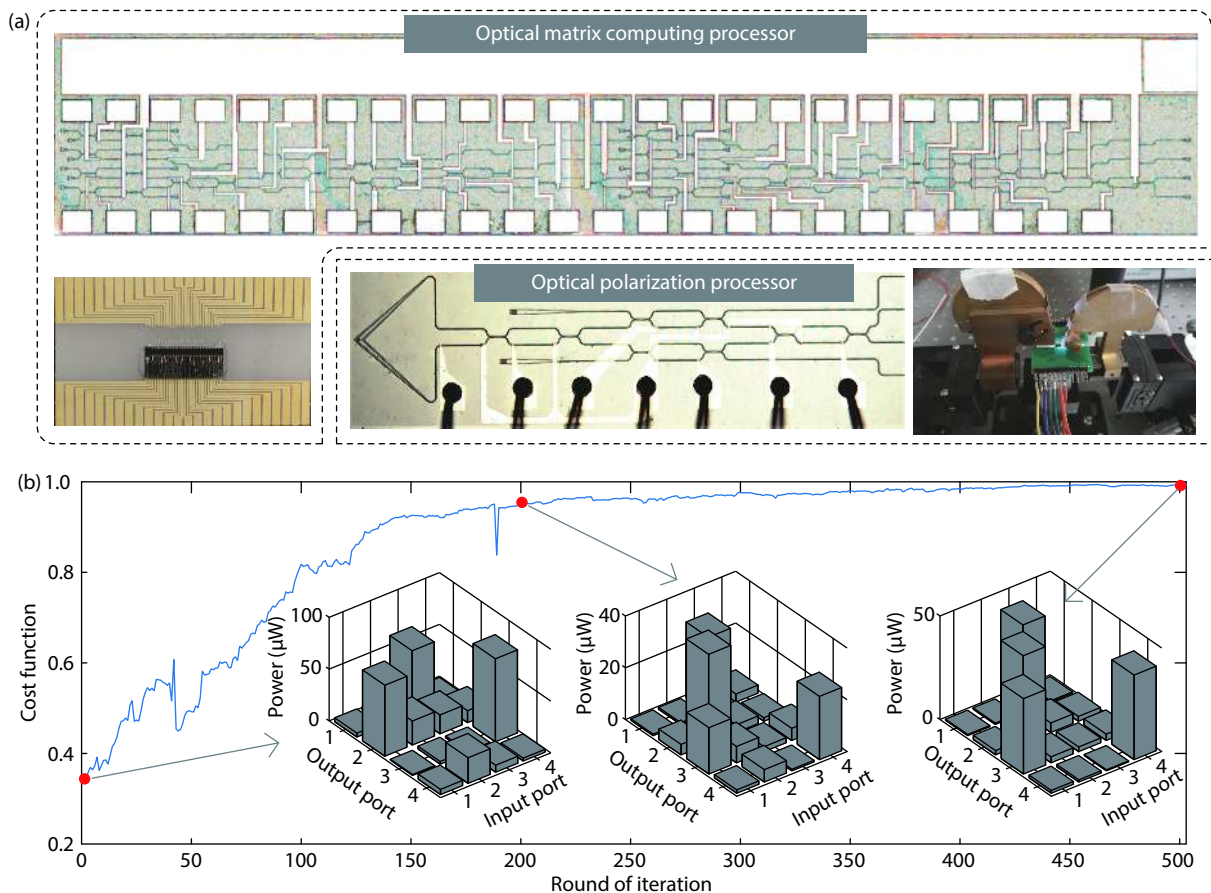


Fig. 17. (Color online) Optical matrix computation and the application for polarization processing. (a) Special-purpose processors for optical matrix computing and polarization processing respectively. (b) Self-configuring example for the smart processors. © [2020] IEEE. Reprinted with permission from Ref. [55].

modulator arrays is illustrated in Figs. 15(a)–15(c)[52]. The input data and convolutional kernel were fed into the modulator arrays to carry out the operation. With the hardware reusing scheme, complicated CNNs can be conducted by the

units. In Fig. 15(d), convolution results on the digital computer and the proposed OCU are shown to support the feasibility.

A more complete optical CNN implementation incorporat-

**S Y Xiang et al.: A review: Photonics devices, architectures, and algorithms for optical neural computing**
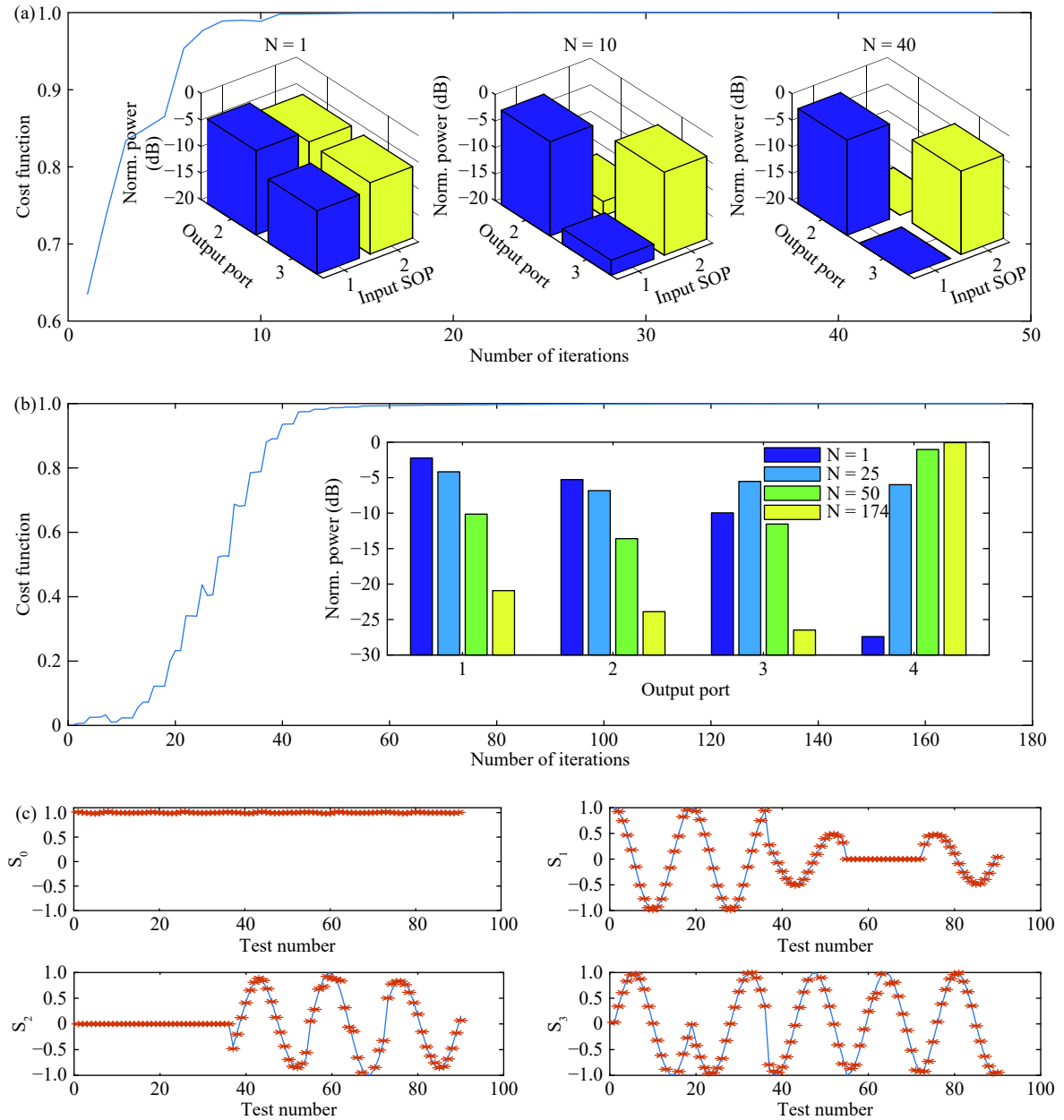
Fig. 18. (Color online) Experimental results for photonic polarization processor chip. (a) Polarization MIMO descrambler. (b) Polarization controller. (c) Polarization analyzer. Reprinted with permission from Ref. [58]. © The Optical Society.

ing patching scheme was demonstrated in[53]. In Figs. 16(a) and 16(b), the introduction of optical delay lines to execute data manipulations promises low latency and power consumption. Meanwhile, wavelength-division-demultiplexing (WDM) was used to improve the computational capacity by parallel wavelength channels. Illustrated by Figs. 16(c)–16(f), the serialized input waveforms of digit 2 and 4 were successful to form delayed copies as the experimental demonstration of optical patching. Consequently, the scale of input modulator arrays was largely cut down.

### 4.3.  Optical matrix computation

Matrix computations form the most widely used computational tools in science and engineering, and are the basic components of neural networks for deep learning. While the electronic matrix computations suffer from limited bandwidth. Alternatively, the optical methods offer a high-speed and low-

loss solution. Optical matrix computation is also essential in the optical neural computing.

The Mech-Zehnder interferometer (MZI) mesh had been demonstrated for optical matrix computation[55, 56]. As shown in Fig. 17(a), the optical matrix computing processor can perform fundamental matrix computations including $XB = C$, $AB = X$ and $AX = C$, where $A$, $B$, $C$ are known matrices, and $X$ is the matrix to be solved. Fig. 17(b) shows an example to self-configure a transmission matrix. An optical PageRank algorithm was further demonstrated based on the matrix computing processor. Furthermore, the optical matrix computation core could be applied for polarization processing[57, 58]. The micrograph of chip is presented in Fig. 17(a) and some experimental results are depicted in Fig. 18. The polarization processor could implement multiple polarization processing functions, including polarization multiple-input-multiple-output (MIMO) descrambler, polarization controller and polarization
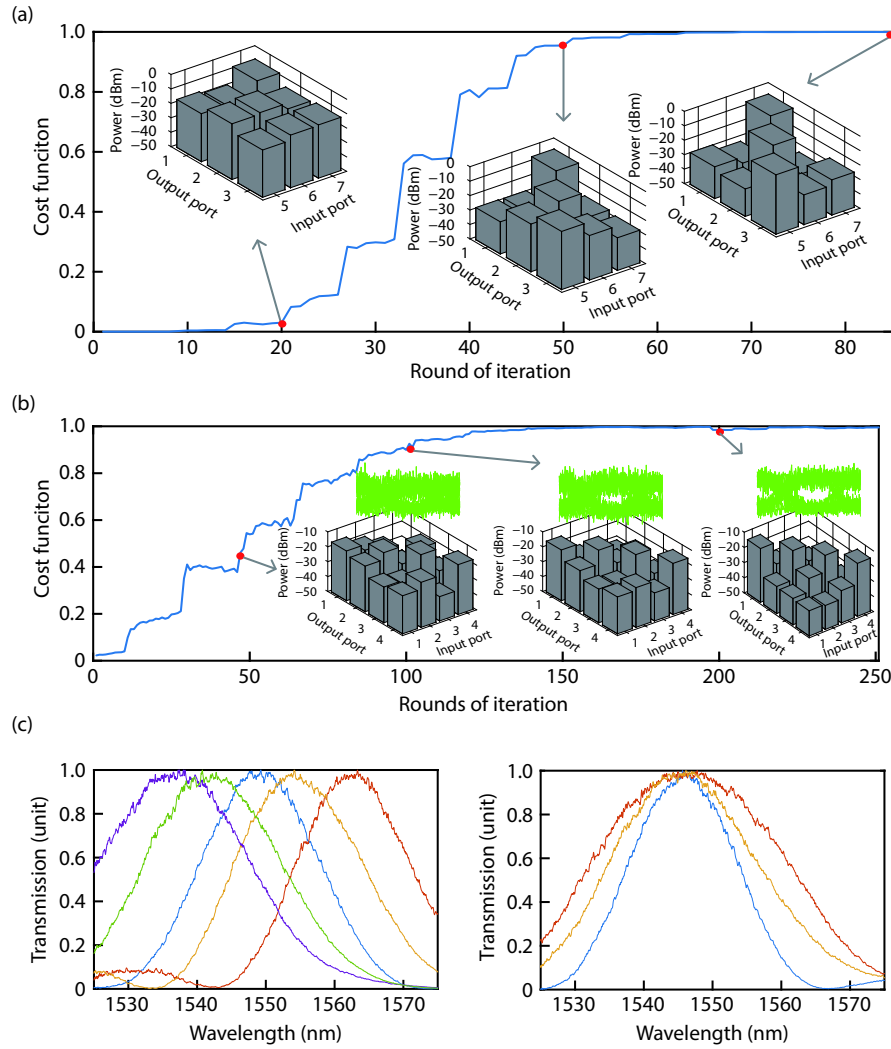
Fig. 19. (Color online) Experimental results for self-configuring optical signal processor. (a) Multichannel optical switching. (b) Optical MIMO descramble. (c) Tunable optical filter. Reprinted with permission from Ref. [59]. © 2017 American Chemical Society.

analyzer, which are the basic building blocks of polarization processing. More functions could be realized by using an additional two-dimensional output grating. A numerical gradient descent algorithm was employed to self-configure and self-optimize these functions. Recently, the 4-port general linear network has been applied for multi-channel optical switching, MIMO descramble and tunable filter by learning strategy[59]. Fig. 19 shows the typical demonstration of the three functions respectively. The works suggested great potential for chip-scale reconfigurable and fully programmable photonic computing and optical signal processors with artificial intelligent algorithm.

### 4.4. Photonic reservoir computing

RC is a brain-inspired computational paradigm originated from recurrent neural network suitable for time series processing[60–62]. In the training process of RC systems, only the output weights are modified, while the input and reservoir weights are fixed randomly. Specifically, the time-delay RC system based on a single nonlinear node with delay feedback has been demonstrated in electronic, optoelectronic, and all optical delay systems[63–65]. In recent years, we have also made some attempts to the time-delay RC via photonics approaches[66–70].

An attempt at the time-delay RC systems based on VCSEL is that we proposed a four-channels RC system based on polarization dynamics in mutually coupled VCSELs[67]. As shown in Fig. 20(a), four channels RC were realized in two orthogonal polarization modes of two VCSELs. The outputs obtained from the four channels were combined into one output for post-processing as displayed in Fig. 20(b). The four-channels RC could produce comparable prediction performance but at a faster information processing rate compared with the one-channel RC as shown in Fig. 20(c).

We also have some attempts at the time-delay RC system based on semiconductor nanolaser (SNL), due to the potential of realizing photonic integrated RC system[69, 70]. For example, a high-speed neuromorphic SNL-based RC system under electrical modulation was proposed[69]. The conceptual scheme of the SNL-based RC system is presented in Fig. 21(a). The numerical simulation results are shown in Fig. 21(b), which show that a larger Purcell factor $F$ and larger spontaneous emission coupling factor $\beta$ could extend the range of high prediction performance of SNL-based RC system.

### 4.5. Photonic reinforcement learning

Reinforcement learning is also a fundamental learning mechanism inspired by the brain[71]. In reinforcement learn-
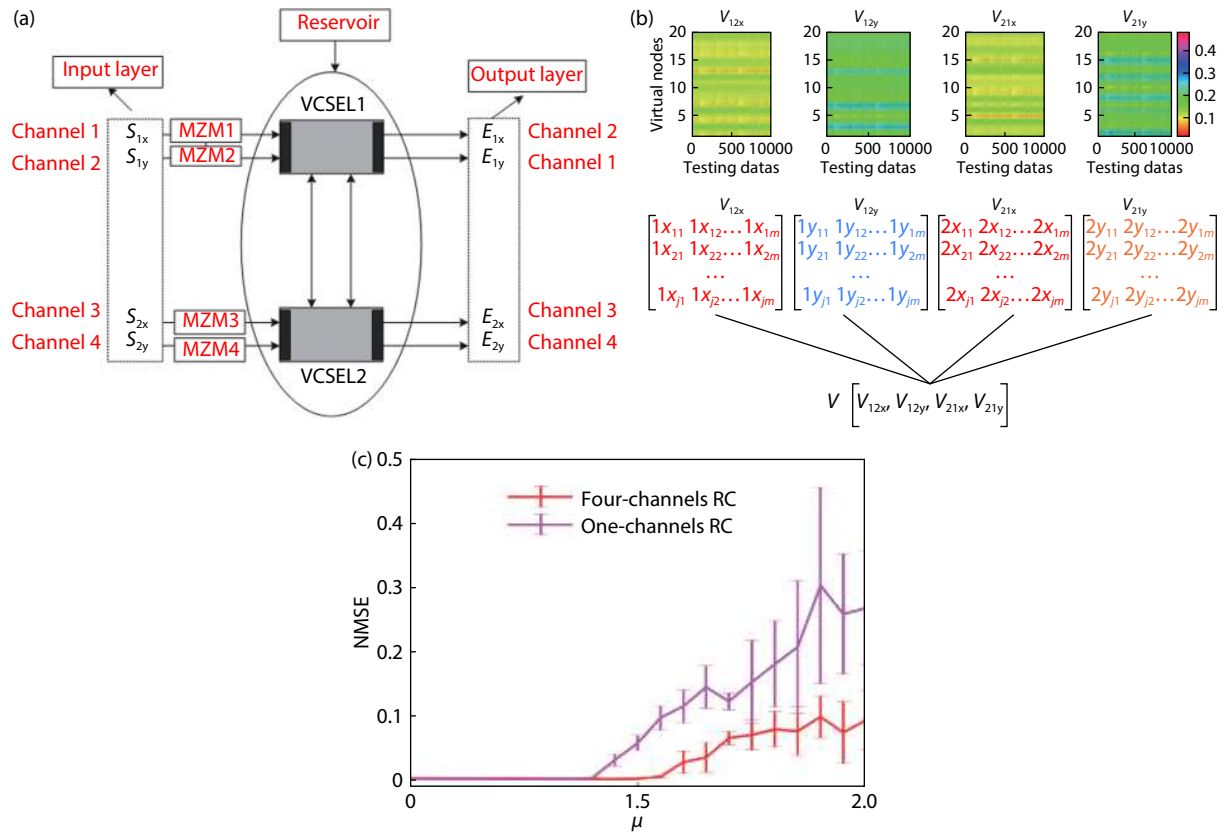
Fig. 20. (Color online) (a) System design of the Four-channels RC based on MDC-VCSELs. (b) The virtual node states matrix for each channel. (c) The NMSE values of Four-channels RC system based on MDC-VCSELs as a function of bias current for Four-channels RC and One-channel RC, respectively. Reprinted with permission from Ref. [67]. © The Optical Society.
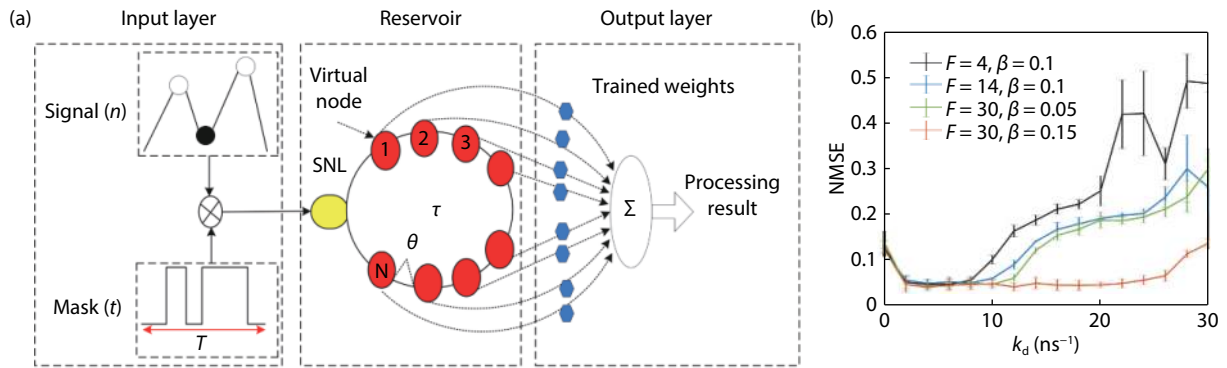


Fig. 21. (Color online) (a) The conceptual scheme of RC based on a semiconductor nanolaser (SNL) with delayed feedback. (b) The NMSE values of SNL-based RC system as a function of the $k_d$ for different $F$ and $\beta$. © [2020] IEEE. Reprinted with permission from Ref. [69].

ing, an agent learns from interaction process with the environment, aims to maximize the benefits via certain learning strategies. Decision-making is a basic component of reinforcement learning, which requires the agent to make decision quickly and accurately in an uncertain and dynamically changing environment[72]. Photonic decision making provides possibilities in applications of ultrafast processing.

The photonic reinforcement learning based on laser chaos with time-delay signature concealment was demonstrated by introducing a phase-modulated Sagnac loop in mutually delay-coupled semiconductor lasers (PMSL-MC)[73], as shown in Fig. 22. The multi-armed bandit problem was solved in parallel with the utilization of dual-channel chaotic signals. The comparison between the PMSL-MC system and

conventional mutually-coupled semiconductor lasers system (CSL-MC) further demonstrated that the system with dual-channels chaotic signals can make decision in parallel and converge faster.

A further parallelized scheme for photonic decision making was experimentally demonstrated in a globally-coupled chaotic semiconductor lasers network as shown in Fig. 23[74]. Triple-channel chaotic signals were applied to solve an 8-armed bandit problem with a parallel architecture given in Fig. 23(b). In Figs. 23(c) and 23(d), the results suggested that the chaotic signals with better time delay signature concealment generally contributed to better decision-making performance. The adaptability of the strategy to environmental change was further demonstrated as in Fig. 23(e). More-
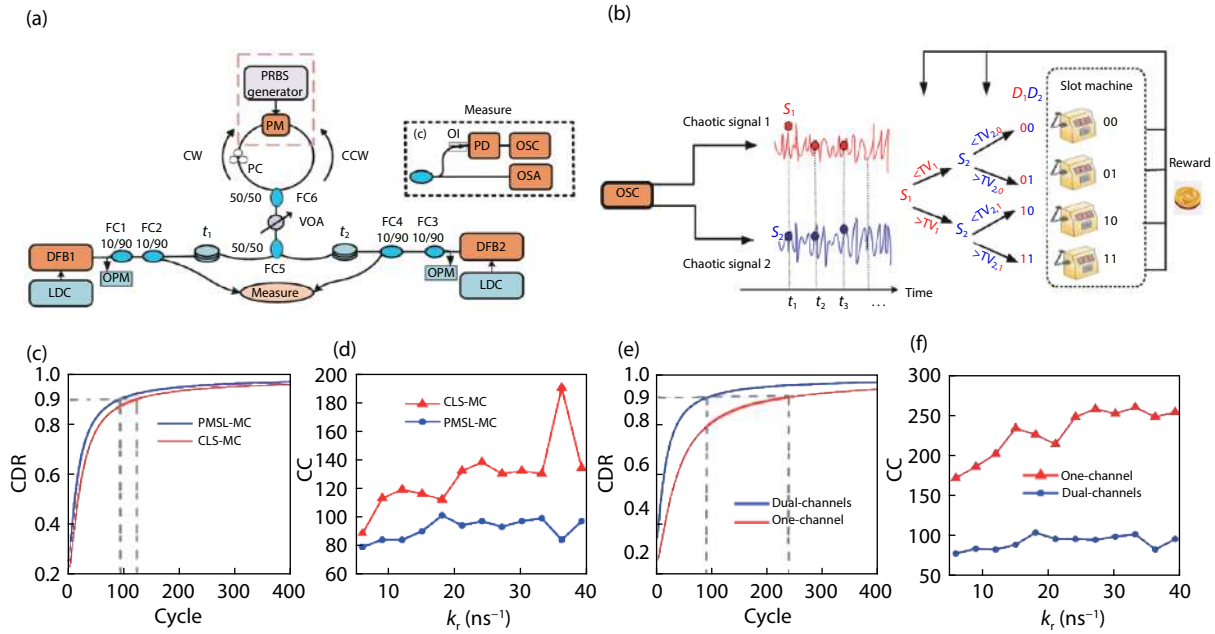
Fig. 22. (Color online) (a) Experimental setup of a dual-channels chaotic system with a phase-modulated Sagnac loop. (b) Architecture for reinforcement learning based on dual-channels laser chaos. (c) The CDR as a function of cycle for the CSL-MC system and for the PMSL-MC system. (d) The convergence cycle (CC), at which the CDR reaches 0.9, as a function of coupling strength for the CSL-MC system and the PMSL-MC system. (e) The CDR as a function of the number of cycles for dual-channels and one-channel in the PMSL-MC system. (f) The CC as a function of coupling strength for dual-channels and one-channel in the PMSL-MC system. Reprinted with permission from Ref. [73]. © The Optical Society.
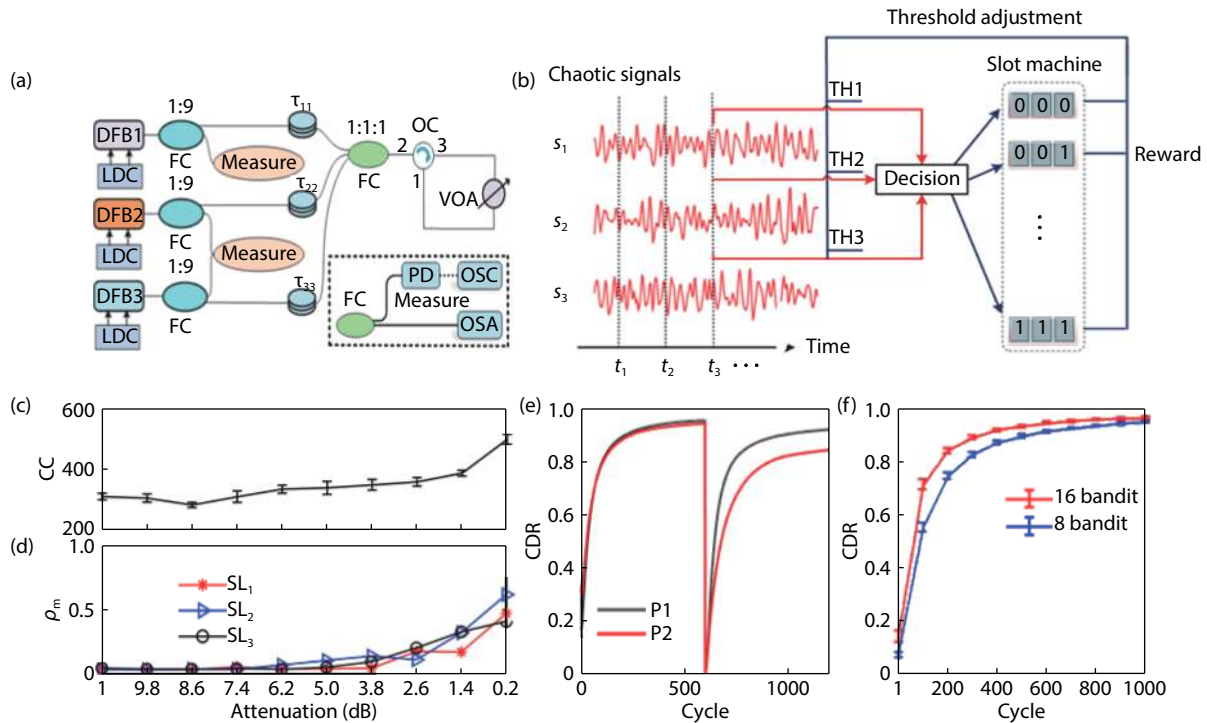


Fig. 23. (Color online) (a) The experimental setup of three globally coupled DFB lasers. (b) A parallel architecture for photonic decision making of 8-armed bandit problem. (c, d) CC and delay concealment as a function of attenuation. (e) The adaptability of the strategy to dynamically changing environment. (f) The scalability to 16-armed problem. Reprinted from Ref. [74]. Copyright (2020) with permission from Chinese Laser Press.

over, such a scheme was also scalable as demonstrated in Fig. 23(f), where both 8-armed and 16-armed bandit problems were solved successfully.

## 5. Conclusion and outlook

We have reviewed some representative photonic neural computing in devices, architectures, and algorithms. To fur-

ther pave the way of photonics neuromorphic computing, there are still some problems that need to be addressed. The optical neuron and synapse are generally designed separately, which results in the different time scales. The optical neuron and synapse with similar time scale have to be further developed to meet up the requirements of on-line training. The design of photonic neural computing system on a

**S Y Xiang et al.: A review: Photonics devices, architectures, and algorithms for optical neural computing**

chip still requires further exploration. Further attempts have to be made to reduce the area and increase the integration level.

Note, at the present stage, we think it may be more realistic to adopt an *ex-situ* training approach for the training process of the photonic neural network. Nevertheless, it is promising to build an integrated hardware photonic neural network for realizing the inference process. At present, the optical neuron based on spiking laser could be readily realized with III–V compound semiconductor technology such as indium phosphide (InP) and gallium arsenide (GaAs), while the weight array could be successfully implemented with silicon waveguides or resonators. It is believed that the rapid development of photonic integrated technologies will lead to a bright future for the field of photonic neural computing. For instance, a hybrid III–V and silicon photonics platform may be a candidate to realize an integrated hardware photonic neural network for inference task[75–84], in which spiking lasers array in a bonded InP layer could be interconnected via a silicon layer[13, 78].

## Acknowledgements

## References

[1]   Moore G E. Cramming more components onto integrated circuits. Electron, 1965, 38(8), 114

[2]   Waldrop M M. The chips are down for Moore's law. Nat News, 2016, 530(7589), 144

[3]   Maass W. Networks of spiking neurons: The third generation of neural network models. Neur Netw, 1997, 10(9), 1659

[4]   Mainen Z F, Sejnowski T J. Reliability of spike timing in neocortical neurons. Science, 1995, 268(5216), 1503

[5]   Hopfield J J. Pattern recognition computation using action potential timing for stimulus representation. Nature, 1995, 376(6535), 33

[6]   Bi G Q, Poo M M. Synaptic modifications in cultured hippocampal neurons: Dependence on spike timing, synaptic strength, and postsynaptic cell type. J Neurosci, 1998, 18(24), 10464

[7]   Abbott L F, Nelson S B. Synaptic plasticity: Taming the beast. Nat Neurosci, 2000, 3, 1178

[8]   Bi G Q, Poo M M. Synaptic modification by correlated activity: Hebb's postulate revisited. Annu Rev Neurosci, 2001, 24, 139

[9]   Schuman C D, Potok T E, Patton R M, et al. A survey of neuromorphic computing and neural networks in hardware. arXiv preprint arXiv: 1705. 06963, 2017

[10]  Roy K, Jaiswal A, Panda P. Towards spike-based machine intelligence with neuromorphic computing. Nature, 2019, 575, 607

[11]  Zhu J D, Zhang T, Yang Y C, et al. A comprehensive review on emerging artificial neuromorphic devices. Appl Phys Rev, 2020, 7, 011312

[12]  Zhang W, Gao B, Tang J, et al. Neuro-inspired computing chips. Nat Electron, 2020, 3, 371

[13]  Prucnal P R, Shastri B J, de Lima T F, et al. Recent progress in semiconductor excitable lasers for photonic spike processing. Adv Opt Photon, 2016, 8(2), 228

[14]  Nahmias M A, Shastri B J, Tait A N, et al. A leaky integrate-and-fire laser neuron for ultrafast cognitive computing. IEEE J Sel Top Quantum Electron, 2013, 19(5), 1800212

[15]  Gholipour B, Bastock P, Craig C, et al. Amorphous metal-sulphide microfibers enable photonic synapses for brain-like computing. Adv Opt Mater, 2015, 5(3), 635

[16]  Cheng Z, Ríos C, Pernice W H P, et al. On-chip photonic synapse. Sci Adv, 2017, 3(9), e1700160

[17]  Feldmann J, Youngblood, Wright N C D, et al. All-optical spiking neurosynaptic networks with self-learning capabilities. Nature, 2019, 569, 208

[18]  Zhuge X, Wang J, Zhuge F. Photonic synapses for ultrahigh-speed neuromorphic computing. Phys Status Solidi RRL, 2019, 13, 1900082

[19]  de Lima T F, Peng H T, Tait A N, et al. Machine learning with neuromorphic photonics. J Lightwave Technol, 2019, 37(5), 1515

[20]  Zou W W, Ma B W, Xu S F, et al. Towards an intelligent photonic system. Sci China Inform Sci, 2020, 63, 160401

[21]  Shastri B J, Tait A N, de Lima T F, et al. Photonics for artificial intelligence and neuromorphic computing. arXiv preprint arXiv: 2011.00111v1, 2020

[22]  Hurtado A, Henning I D, Adams M J. Optical neuron using polarization switching in a 1550 nm-VCSEL. Opt Express, 2010, 18(24), 25170

[23]  Coomans W, Gelens L, Beri S, et al. Solitary and coupled semiconductor ring lasers as optical spiking neurons. Phys Rev E, 2011, 84(3), 036209

[24]  Hurtado A, Schires K, Henning I, et al. Investigation of vertical cavity surface emitting laser dynamics for neuromorphic photonic systems. Appl Phys Lett, 2012, 100(10), 103703

[25]  Xiang S Y, Wen A J, Pan W. Emulation of spiking response and spiking frequency property in VCSEL-based photonic neuron. IEEE Photonics J, 2016, 8(5), 1504109

[26]  Robertson J, Deng T, Javaloyes J. Controlled inhibition of spiking dynamics in VCSELs for neuromorphic photonics: theory and experiments. Opt Lett, 2017, 42(8), 1560

[27]  Xiang S Y, Zhang Y H, Guo X X, et al. Cascadable neuron-like spiking dynamics in coupled VCSELs subject to orthogonally polarized optical pulse injection. IEEE J Sel Top Quantum Electron, 2017, 23(6), 1700207

[28]  Deng T, Robertson J, Hurtado A. Controlled propagation of spiking dynamics in vertical-cavity surface-emitting lasers: towards neuromorphic photonic networks. IEEE J Sel Top Quantum Electron, 2017, 23(6), 1800408

[29]  Xiang S Y, Zhang Y H, Guo X X, et al. Photonic generation of neuron-like dynamics using VCSELs subject to double polarized optical injection. J Lightwave Technol, 2018, 36(19), 4227

[30]  Deng T, Robertson J, Wu Z M, et al. Stable propagation of inhibited spiking dynamics in vertical-cavity surface-emitting lasers for neuromorphic photonic networks. IEEE Access, 2018, 6, 67951

[31]  Zhang Y H, Xiang S Y, Guo X X, et al. Polarization-resolved and polarization-multiplexed spike encoding properties in photonic neuron based on VCSEL-SA. Sci Rep, 2018, 8, 16095

[32]  Zhang Y H, Xiang S Y, Gong J K, et al. Spike encoding and storage properties in mutually coupled vertical-cavity surface-emitting lasers subject to optical pulse injection. Appl Opt, 2018, 57(7), 1731

[33]  Zhang Y H, Xiang S Y, Guo X X, et al. All-optical inhibitory dynamics in photonic neuron based on polarization mode competition in a VCSEL with an embedded saturable absorber. Opt Lett, 2019, 44(7), 1548

[34]  Xiang S Y, Ren Z, Zhang Y, et al. All-optical neuromorphic XOR operation with inhibitory dynamics of a single photonic spiking neuron based on VCSEL-SA. Opt Lett, 2020, 45(5), 1104

[35]  Xiang S Y, Zhang Y H, Gong J K, et al. STDP-based unsupervised spike pattern learning in a photonic spiking neural network with VCSELs and VCSOAs. IEEE J Sel Top Quantum Electron, 2019, 25(6), 1700109

[36]  Robertson J, Wade, Kopp E Y, et al. Toward neuromorphic photonic networks of ultrafast spiking laser neurons. IEEE J Sel Top

Quantum Electron, 2020, 26(1), 7700715

[37] Ma B W, Zou W W. Demonstration of a distributed feedback laser diode working as a graded-potential-signaling photonic neuron and its application to neuromorphic information processing. Sci China Inform Sci, 2020, 63, 160408

[38] Ma B W, Chen J P, Zou W W. A DFB-LD-based photonic neuromorphic network for spatiotemporal pattern recognition. Proceedings of Optical Fiber Communication Conference, 2020, M2K.2

[39] Xiang S Y, Ren Z X, Song Z W, et al. Computing primitive of fully-VCSELs-based all-optical spiking neural network for supervised learning and pattern classification. IEEE Trans Neural Netw Learn Syst, 2020, in press

[40] Toole R, Fok M P. Photonic implementation of a neuronal algorithm applicable towards angle of arrival detection and localization. Opt Express, 2015, 23(12), 16133

[41] Ren Q S, Zhang Y L, Wang R, et al. Optical spike-timing-dependent plasticity with weight-dependent learning window and reward modulation. Opt Express, 2015, 23(19), 25247

[42] Toole R, Tait A N, de Lima T F, et al. Photonic implementation of spike-timing-dependent plasticity and learning algorithms of biological neural systems. J Lightwave Technol, 2016, 34(2), 470

[43] Li Q, Wang Z, Le Y S, et al. Optical implementation of neural learning algorithms based on cross-gain modulation in a semiconductor optical amplifier. Proc SPIE, 2016, 10019, 2245976

[44] Xiang S Y, Gong J K, Zhang Y H, et al. Numerical implementation of wavelength-dependent photonic spike timing dependent plasticity based on VCSOA. IEEE J Quantum Electron, 2018, 54(6), 8100107

[45] Lima T, Shastri B J, Tait A N, et al. Progress in neuromorphic photonics. Nanophotonics, 2017, 6(3), 577

[46] Song S, Kim J, Kwon S M, et al. Recent progress of optoelectronic and all-optical neuromorphic devices: a comprehensive review of device structures, materials, and applications. Adv Intell Syst, 2020, 2000119

[47] Xiang S Y, Han Y N, Guo X X, et al. Real-time optical spike-timing dependent plasticity in a single VCSEL with dual-polarized pulsed optical injection. Sci China Inform Sci, 2020, 63, 160405

[48] Song Z W, Xiang S Y, Ren Z X, et al. Spike sequence learning in a photonic spiking neural network consisting of VCSELs-SA with supervised training. IEEE J Sel Top Quantum Electron, 2020, 26(5), 1700209

[49] Song Z W, Xiang S Y, Ren Z X, et al. Photonic spiking neural network based on excitable VCSELs-SA for sound azimuth detection. Opt Express, 2020, 28(2), 1561

[50] Zhang Y H, Xiang S Y, Guo X X, A. Wen, et al The winner-take-all mechanism for all-optical systems of pattern recognition and max-pooling operation. J Lightwave Technol, 2020, 38(18), 5071

[51] Wang S H, Xiang S Y, Han G Q, et al. Photonic associative learning neural network based on VCSELs and STDP. J Lightwave Technol, 2020, 38(17), 4691

[52] Xu S F, Wang J, Wang R, et al. High-accuracy optical convolution unit architecture for convolutional neural networks by cascaded acousto-optical modulator arrays. Opt Express, 2019, 27, 19778

[53] Xu S F, Wang J, Zou W W. Optical patching scheme for optical convolutional neural networks based on wavelength-division multiplexing and optical delay lines. Opt Lett, 2020, 45, 3689

[54] Xu S F, Zou X T, Ma B W, et al. Deep-learning-powered photonic analog-to digital conversion. Light Sci Appl, 2019, 8(1), 66

[55] Zhou H L, Zhao Y H, Xu G X, et al. Chip-scale optical matrix computation for PageRank algorithm. IEEE J Sel Top Quantum Electron, 2020, 26, 8300910

[56] Zhao Y H, Zhou H L, Dong J J. An optical processor for matrix computation on silicon-on-insulator. International Conference on Photonics in Switching and Computing OptoElectronics and Communications Conference, 2019

[57] Zhou H L, Zhao Y H, Wei Y X, et al. All-in-one silicon photonic polar-

[58] Zhou H L, Zhao Y H, Wei Y X, et al. Multipurpose photonic polarization processor chip. Asia Communications and Photonics Conference, 2019, M4A.229

[59] Zhou H L, Zhao Y H, Wang X, et al. Self-configuring and reconfigurable silicon photonic signal processor. ACS Photonics, 2020, 7, 792

[60] Maass W, Natschlager T, Markram H. Real-time computing without stable states: a new framework for neural computation based on perturbations. Neur Comput, 2002, 14(11), 2531

[61] Maass W, Natschlager T, Markram H. Fading memory and kernel properties of generic cortical microcircuit models. J Physiol-Paris, 2004, 98(4–6), 315

[62] Lukosevicius M, Jaeger H. Reservoir computing approaches to recurrent neural network training. Comput Sci Rev, 2009, 3(3), 127

[63] Guy V D S, Brunner D, Soriano M C. Advances in photonic reservoir computing. Nanophotonics, 2017, 6(3), 561

[64] Brunner D, Penkovsky B, Marquez B A, et al. Tutorial: Photonic neural networks in delay systems. J Appl Phys, 2018, 124(15), 152004

[65] Tanaka G, Yamane T, Héroux J B, et al. Recent advances in physical reservoir computing: A review. Neur Netw, 2019, 115, 100

[66] Guo X X, Xiang S Y, Zhang Y H, et al. Polarization multiplexing reservoir computing based on a VCSEL with polarized optical feedback. IEEE J Sel Top Quantum Electron, 2020, 26(1), 1700109

[67] Guo X X, Xiang S Y, Zhang Y H, et al. Four-channels reservoir computing based on polarization dynamics in mutually coupled VCSELs system. Opt Express, 2019, 27(16), 23293

[68] Guo X X, Xiang S Y, Zhang Y H, et al. Enhanced memory capacity of a neuromorphic reservoir computing system based on a VCSEL with double optical feedbacks. Sci China Inf Sci, 2020, 63(6), 160407

[69] Guo X X, Xiang S Y, Zhang Y H, et al. High-speed neuromorphic reservoir computing based on a semiconductor nanolaser with optical feedback under electrical modulation. IEEE J Sel Top Quantum Electron, 2020, 26(5), 1500707

[70] Guo X X, Xiang S Y, Y. Qu, et al Enhanced prediction performance of a neuromorphic reservoir computing using a semiconductor nanolaser with double phase conjugate feedbacks. J Lightwave Technol, 2021, 39(1), 129

[71] Sutton R S, Barto A G. Reinforcement learning: an introduction. The MIT Press Cambridge, Massachusetts London, England, 1998, 712192

[72] Naruse M, Mihana T, Hori H, et al. Scalable photonic reinforcement learning by time-division multiplexing of laser chaos. Sci Rep, 2018, 8(1), 10890

[73] Ma Y T, Xiang S Y, Guo X X, et al. Time-delay signature concealment of chaos and ultrafast decision making in mutually coupled semiconductor lasers with a phase-modulated Sagnac loop. Opt Express, 2020, 28, 1665

[74] Han Y N, Xiang S Y, Wang Y, et al. Generation of multi-channel chaotic signals with time delay signature concealment and ultrafast photonic decision making based on globally-coupled semiconductor lasers network. Photonics Res, 2020, 8(11), 1792

[75] Zhou Z, Tu Z, Yin B, et al. Development trends in silicon photonics. Chin Opt Lett, 2013, 11(1), 012501

[76] Zhou Z P, Yin B, Michel J. On-chip light sources for silicon photonics. Light Sci Appl, 2015, 4, e358

[77] Atabaki A H, Moazeni S, Pavanello F, et al. Integrating photonics with silicon nanoelectronics for the next generation of systems on a chip. Nature, 2018, 556, 349

[78] Billah M R, Blaicher M, Hoose T, et al. Hybrid integration of silicon photonics circuits and InP lasers by photonic wire bonding. Optica, 2018, 5, 876

[79] Guo X H, He A, Su Y K. Recent advances of heterogeneously integrated IIIV laser on Si. J Semicond, 2019, 40(10), 101304

[80] Bai B W, Shu H W, Wang X J, et al. Towards silicon photonic neur-

al networks for artificial intelligence. Sci China Inf Sci, 2020, 63(6), 160403

[81] Bao S Y, Wang Y, Lina K, et al. A review of silicon-based wafer bonding processes, an approach to realize the monolithic integration of Si-CMOS and IIIV-on-Si wafers. J Semicond, 2020, in press

[82] Ruan Z L, Zhu Y T, Chen P X, et al. Efficient hybrid integration of long-wavelength VCSELs on silicon photonic circuits. J Lightwave Technol, 2020, 38(18), 5100

[83] Li Y Y, Wang Y, Yang D R, et al. Recent progress on optoelectronic synaptic devices. Sci Sin Inform, 2020, 50, 892

[84] Wetzstein G, Ozcan A, Gigan S, et al. Inference in artificial intelligence with deep optics and photonics. Nature, 2020, 588, 39

**Shuiying Xiang** was born in Ji'an, China, in 1986. She received the Ph.D. degree from Southwest Jiaotong University, Chengdu, China, in 2013. She is currently a Professor with State Key Laboratory of Integrated Service Networks, Xidian University, Xi'an, China. She is the author or coauthor of more than 100 research papers. Her research interests include vertical cavity surface-emitting lasers, neuromorphic photonic systems, brain-inspired information processing, chaotic optical communication, and semiconductor lasers dynamics.

**Yue Hao** was born in the city of Chongqing, China, in 1958. He received the Ph.D. degree from Xi'an Jiao tong University, Xi'an, China, in 1991. He is currently a Professor at State Key Discipline Laboratory of Wide Bandgap Semiconductor Technology, the School of Microelectronics, Xidian University, Xi'an, China. His research interests include wide forbidden band semiconductor materials and devices, semiconductor device reliability physics and failure mechanism, terahertz semiconductor materials and device.